Interleukin-4 induces CD11c^{+} microglia leading to amelioration of neuropathic pain in mice

Keita Kohno[1], Ryoji Shirasaka[1], Keita Hirose[1], Takahiro Masuda[2], Makoto Tsuda[1,3,4]*

Affiliations

[1] Department of Molecular and System Pharmacology, Graduate School of Pharmaceutical Sciences, Kyushu University, 3-1-1 Maidashi, Higashi-ku, Fukuoka 812-8582, Japan

[2] Division of Molecular Neuroimmunology, Medical Institute of Bioregulation, Kyushu University, 3-1-1 Maidashi, Higashi-ku, Fukuoka 812-8582, Japan

[3] Kyushu University Institute for Advanced Study, 744 Motooka Nishi-ku, Fukuoka 819-0395, Japan

[4] Lead contract

*Correspondence: Makoto Tsuda, Ph.D.; **TEL:** 81-92-642-6628, **FAX:** 81-92-642-6566, **Email:** E-mail: tsuda@phar.kyushu-u.ac.jp

Abstract

Neuropathic pain, a debilitating chronic pain condition, is a major clinical challenge. The pleiotropic cytokine interleukin-4 (IL-4) has been shown to suppress neuropathic pain in rodent models, but its underlying mechanism remains unclear. Here, we show that intrathecal administration of IL-4 to mice with spinal nerve transection (SpNT) increased the number of CD11c$^+$ microglia (a microglia subset important for pain remission) in the spinal dorsal horn (SDH) and that this effect of IL-4 was essential for its ameliorating effect on SpNT-induced pain hypersensitivity. Furthermore, in mice with spared nerve injury (SNI), another model in which pain remission does not occur, the emergence of CD11c$^+$ SDH microglia was curtailed, but intrathecal IL-4 increased their emergence and ameliorated pain hypersensitivity in a CD11c$^+$ microglia-dependent manner. Our study reveals a mechanism by which intrathecal IL-4 ameliorates pain hypersensitivity after nerve injury and provides evidence that IL-4 increases CD11c$^+$ microglia with a function that ameliorates neuropathic pain.

Introduction

Neuropathic pain is a debilitating chronic pain condition that results from injury or disease of the somatosensory system. Since chronic pain is refractory to currently available treatments, the development of effective treatments is a major clinical challenge [1,2]. Accumulating evidence from studies using models of neuropathic pain indicates that peripheral nerve injury causes various inflammatory responses in the nervous system that critically contribute to the development of neuropathic pain [3,4]. Especially, pro-inflammatory cytokines [e.g., interleukin-1β (IL-1β), IL-6 and tumor necrosis factor α (TNFα)] produced by various non-neuronal cells such as macrophages at injured nerves and dorsal root ganglion (DRG), and glial cells (mainly microglia and astrocytes) in the spinal dorsal horn (SDH) modulate function of primary afferent sensory neurons and SDH neurons, leading to an increase in the excitability of pain signaling neural pathway [3–6]. Along with these findings, much attention has been paid to the pain-relieving role of anti-inflammatory cytokines [7]. These include IL-10, the role of which in chronic pain has been extensively studied [7]. Another anti-inflammatory cytokine with pain-relieving effects in diverse models, including neuropathic pain, is IL-4. Intraplantar or systemic administration of IL-4 has been shown to attenuate pain behavioral responses to bradykinin [8], carrageenin [8], TNFα [8], zymosan [9] and acetic acid [9] in normal animals. In models of neuropathic pain, single or repeated administration of IL-4 around the injured sciatic nerve reduced behavioral pain hypersensitivity [10–12]. These effects of IL-4 have been proposed to involve a decrease in the production of inflammatory mediators [11], polarization of macrophages toward an anti-inflammatory phenotype at injured nerves [10,11], increases in the production and release of IL-10 [11] and opioid

peptides [10,12] from macrophages, and inhibition of the increased action potentials of DRG neurons [13]. In addition to the diverse actions of IL-4 at the peripheral level, the central nervous system, including the spinal cord, is recognized as an important locus of action of IL-4 in pain control. Intrathecal administration of IL-4 prevents the development of mechanical pain hypersensitivity in several neuropathic pain models [13,14]. The target cells for the action of IL-4 intrathecally administered could be microglia since, within the SDH of nerve-injured rats, IL-4 receptor α chain (IL-4Rα) is predominantly expressed in microglia [14]. In line with this, intrathecal IL-4 activates signal transducer and activator of transcription 6 (STAT6; an intracellular signal transduction molecule downstream of IL-4Rα) in SDH microglia [14]. Intrathecal IL-4 or other manipulation to increase spinal IL-4 during early phase after nerve injury suppresses cellular indexes for reactive microglia [14], IL-1β and Prostaglandin E2 release, and microglial p38 phosphorylation [15], all of which are required to develop pain hypersensitivity [4]. In addition to the effect of IL-4 on pain development, it is noteworthy that intrathecal administration of IL-4 during the late phase (e.g., 2 weeks or later after nerve injury) leads to recovery from a behavioral pain-hypersensitive state that develops following nerve injury [14]. Despite the remarkable therapeutic potential of spinal IL-4 for ameliorating established neuropathic pain, little is known about its mechanism of action. Given that the reactive states of microglia occur early after nerve injury (e.g., cell number and expression of proinflammatory genes) and subside in the late phase [4,16,17], it is possible that the pain-resolving effect of IL-4 involves a mechanism other than the previously reported suppression of inflammatory responses in activated microglia.

In this study, using two different models of neuropathic pain, we demonstrated that

intrathecally administered IL-4 during the late phase changes microglia to a CD11c$^+$ state, which has recently been shown to be necessary for the spontaneous remission of behavioral hypersensitivity associated with neuropathic pain [18], and, importantly, that this is required for the pain-relieving effect of intrathecal IL-4. Consequently, our findings uncover a mechanism for the ameliorating effect of spinal IL-4 on already-developed neuropathic pain and provide evidence at a preclinical level that IL-4 could induce the emergence of CD11c$^+$ microglia with a function that resolves neuropathic pain.

Results

Intrathecal treatment of IL-4 increases CD11c$^+$ microglia in the SDH and alleviates pain hypersensitivity after SpNT

To examine the effect of IL-4 on the behavioral remission of neuropathic pain, we used mice with spinal nerve transection (SpNT; a model of neuropathic pain [19,20]) and repeated the administration of IL-4 to their intrathecal spaces from day 14 post-SpNT, when the paw withdrawal threshold (PWT) decreased (indicating that mechanical pain hypersensitivity had been developed) (Fig. 1*A*). Intrathecal treatment with IL-4 increased the PWT in the hindpaw ipsilateral (but not contralateral) to the SpNT (Fig. 1*A*). Notably, this behavioral remission of neuropathic mechanical hypersensitivity persisted for at least 5 days after the last intrathecal injection of IL-4. Because we previously showed that CD11c$^+$ microglia emerging in the SDH after SpNT are necessary for the spontaneous remission of pain behavior that gradually occurs around 3 weeks after nerve injury [18], we explored the mechanism of action of spinal IL-4 with a focus on

CD11c$^+$ microglia in the SDH. In *Itgax-Venus* mice, in which CD11c$^+$ cells are visualized using the fluorescent protein Venus [18,21], SpNT increased the number of Venus$^+$ (CD11c$^+$) cells in the SDH ipsilateral to the injury (Fig. 1*B*). Consistent with our previous data [18], almost all CD11c$^+$ cells were immunohistochemically positive for ionized calcium-binding adapter molecule 1 (IBA1) and the purinergic P2Y12 receptor (P2Y12R) (Fig. 1*B* and *C*), which are markers for myeloid cells and microglia, respectively [22,23]. We found that intrathecal administration of IL-4 to SpNT mice enhanced the increase in CD11c$^+$ cells in the SDH (Fig. 1*B-D*). These cells also expressed both IBA1 and P2Y12R (Fig. 1*B* and *C*), indicating that CD11c$^+$ cells increased by intrathecal IL-4 were microglia. Quantitative flow cytometry analysis revealed a significant increase in CD11c$^+$ microglia in the SDH of IL-4-treated SpNT mice (Fig. 1*D*). In contrast, IL-4 did not significantly change the total number of microglia in the SDH (Fig. 1*D*). In addition, intrathecal IL-4 did not induce infiltration of CD169$^+$ monocytes/macrophages into the SDH (Figure 1—figure supplement 1A). These findings suggest that CD11c$^+$ microglia may be involved in the mechanism by which intrathecal treatment with IL-4 attenuates pain hypersensitivity.

IL-4-induced remission of pain hypersensitivity requires spinal CD11c$^+$ microglia

To determine whether CD11c$^+$ microglia are required for pain remission induced by IL-4, we used *Itgax-DTR-EGFP* mice in which the diphtheria toxin (DTX) receptor (DTR) and enhanced green fluorescence protein (EGFP) are expressed on CD11c$^+$ cells [18,24], and administered DTX intrathecally to these mice to deplete CD11c$^+$ microglia in the spinal cord. Intrathecal IL-4 also induced behavioral remission of mechanical hypersensitivity in *Itgax-DTR-EGFP* mice, but the pain-reducing effect was eliminated by intrathecal

injection of DTX on day 17 post-SpNT (Fig. 2*A*). The depletion of EGFP$^+$ (CD11c$^+$) microglia in the SDH by DTX injection was confirmed (Fig. 2*B*), indicating the necessity of spinal CD11c$^+$ microglia for the pain-relieving effect of intrathecal IL-4. IL-4 also alleviated pain hypersensitivity in female mice, which was also dependent on CD11c$^+$ microglia (Fig. 3). In addition to SDH, CD11c$^+$ cells have been shown to be present at the site of injury and in the DRG [18]. Thus, we examined the involvement of CD11c$^+$ cells in the DRG in the pain-relieving effect of intrathecal IL-4 using our previously reported strategy that enables the selective depletion of CD11c$^+$ cells in the periphery [18]. The intraperitoneal administration of DTX at a low dose (2 ng/g mouse) in SpNT mice treated with IL-4 on day 17 efficiently eliminated CD11c$^+$ cells (also positive for IBA1) in the DRG on day 18 (Fig. 4*A*). However, the number of CD11c$^+$ microglia in the SDH were not significantly different between the PBS- and DTX-treated groups (Fig. 4B). Under these conditions, we found that the elevated PWT observed in IL-4-treated mice on day 17 did not change 1 day after intraperitoneal administration of DTX (day 18) (Fig. 4C), suggesting that CD11c$^+$ cells in the DRG are not involved in the IL-4-induced alleviating effect on neuropathic pain. Altogether, these data indicate that intrathecally administered IL-4 induces spinal microglia to be in a CD11c$^+$ state, and that this induction is necessary for the ameliorating effect of IL-4 on neuropathic pain.

CD11c$^+$ microglia appearance in the SDH is blunted in SNI model

To extend the therapeutic potential of CD11c$^+$ microglia induced by IL-4 in neuropathic pain, we employed another model of neuropathic pain [speared nerve injury (SNI); transection of tibial and common peroneal nerves] [25]. Consistent with previous data [25],

SNI induced a long-lasting pain-hypersensitive state without spontaneous remission, at least until the last day of testing (day 56 post-SNI) (Fig. 5*A*), which was in stark contrast to the time course of pain hypersensitivity in the SpNT model. We found that the number of CD11c^{+} microglia in the SDH at 14 days after nerve injury was lower in the SNI model than in the SpNT model (Fig. 5*B*). Quantitative analysis by flow cytometry confirmed that there were fewer CD11c^{+} SDH microglia in the SNI mice (Fig. 5*C*). A blunted appearance was also observed on days 35 and 56 post-SNI. In contrast, the total number of microglia in the SDH was comparable between the two models at all time points tested, suggesting an impairment of the nerve injury-induced appearance of CD11c^{+} microglia in the SNI model. Furthermore, insulin-like growth factor 1 (IGF1) has been identified as a factor that is highly expressed in CD11c^{+} microglia and is necessary for their pain-remitting effect [18]. We quantified *Igf1* mRNA expression in the spinal tissue or fluorescence-activated cell sorting (FACS)-isolated SDH microglia from nerve-injured mice (Fig. 6). While *Igf1* expression in sorted microglia increased in both models after injury, its levels were lower in microglia from SNI mice than in those from SpNT mice (Fig. 6*D*). In addition, an increase in *Igf1* mRNA expression in the tissue homogenate of the upper half of the SDH, where CD11c^{+} microglia accumulate [18], was not observed in tissues from the SNI model (Fig. 6*E*). Moreover, in FACS-isolated CD11c^{high} SDH microglia that highly expressed IGF1, the expression of *Igf1* mRNA was significantly lower in the SNI model (Fig. 6*F*). Thus, given that either the depletion of CD11c^{+} microglia or knockout of their IGF1 prevents the spontaneous remission of pain in the SpNT model [18], the long-lasting pain-hypersensitive state in the SNI model could be related to the blunted increase in CD11c^{+} microglia in the SDH and their lower

expression of IGF1.

IL-4 alleviates SNI-induced pain hypersensitivity in CD11c$^+$ microglia- and IGF1-dependent manners

Based on the above findings, we tested whether IL-4 could increase the number of CD11c$^+$ microglia and resolve pain hypersensitivity in the SNI model. Intrathecal treatment with IL-4 in SNI mice from day 14 to day 16 significantly increased the number of CD11c$^+$ microglia on day 21, almost all of which were positive for IBA1 and P2Y12R (Fig. 7*A*-*C*). Similar to the data obtained for SpNT mice, the total number of microglia in the SDH were not significantly different between PBS- and IL-4-treated SNI mice (Fig. 7*C*). Behaviorally, intrathecal IL-4 treatment alleviated the SNI-induced mechanical hypersensitivity (Fig. 7*D*). Furthermore, the depletion of CD11c$^+$ microglia in the SDH of IL-4-treated SNI mice by intrathecal administration of DTX on day 17 negated the ameliorating effect of IL-4 on pain hypersensitivity (Fig. 8*A* and *B*). Moreover, the IL-4's effect was not observed in *Cx3cr1*$^{CreERT2/+}$;*Igf1*$^{flox/flox}$ mice treated with tamoxifen (Fig. 8*C*), a treatment that enables selective knockout of the *Igf1* gene in tissue-resident *Cx3cr1*$^+$ cells [26], the majority of which are microglia in the SDH [18]. Overall, intrathecally administered IL-4 exhibited a pain-remitting effect in the SNI model, which was dependent on CD11c$^+$ microglia and IGF1.

Discussion

Increasing evidence indicates that following peripheral nerve injury microglia in the SDH

causes significant changes in morphology, cell number, transcriptional and translational activities, and function [4,17,27–29]. Numerous studies have shown that these changes occurring in the early phase after nerve injury are necessary for the development of neuropathic pain [4,28–31]. In contrast to their role, we have recently shown that some SDH microglia in the later phase are changed into CD11c$^+$ states with different transcriptional and functional profiles and that these microglia are required for spontaneous remission of neuropathic pain [18]. Thus, CD11c$^+$ microglia are attracting attention as a potential target for future analgesics [32,33]. In this study, we demonstrated for the first time that CD11c$^+$ microglia are an essential target of IL-4 administered intrathecally to induce the behavioral remission of pain hypersensitivity. The pharmacological effect of intrathecal IL-4 appears to be mediated by its direct action on spinal microglia, as the expression of IL-4Rα in the SDH has been shown to be predominant in microglia after nerve injury [14]. This is also supported by the data that activation of STAT6 (the downstream molecule of IL-4Rα) after intrathecal IL-4 selectively occurs in spinal microglia [14] and that primary cultured microglia treated with IL-4 become CD11c$^+$ and express IGF1 [34–36]. Furthermore, based on our data showing that IL-4 increased the number of CD11c$^+$ microglia without affecting the total number of microglia, it is conceivable that IL-4 acts on microglia and changes their state to CD11c$^+$ microglia (rather than the proliferation of CD11c$^+$ microglia themselves), leading to behavioral remission of neuropathic pain.

Intrathecal IL-4 administration also increased CD11c$^+$ microglia in the SDH contralateral to SpNT but did not change the PWT in the contralateral hindpaw. This gap seems to be related to the selective effect of CD11c$^+$ microglia and their factors (especially IGF1) on pathologically heightened pain sensitivity. In fact, depletion of

CD11c^{+} spinal microglia and intrathecal administration of IGF1 do not elevate pain threshold of the contralateral hindpaw [18].

In addition to SDH, the peripheral effects of IL-4 on neuropathic pain have been reported in several pain models. IL-4 applied to injured peripheral nerves, such as sciatic nerves, ameliorates neuropathic mechanical hypersensitivity [11]. In sciatic nerves, IL-4Rα expression is upregulated in macrophages that accumulate in injured nerves [11]. Intrathecally administered IL-4 may affect cells in the DRG, since chemokine (C-C motif) receptor 2 (CCR2)$^{+}$ monocytes were increased in the capsule of the DRG after IL-4 treatment (Figure 1—figure supplement 1B). The involvement of these monocytes in the DRG in IL-4-induced alleviation of neuropathic pain is unclear and warrants further investigation. However, our findings obtained from mice with depletion of CD11c^{+} IBA1^{+} cells (presumably macrophages) in the DRG (but not SDH) suggest that the cells required for intrathecal IL-4 to ameliorate pain hypersensitivity are CD11c^{+} microglia in the SDH, but not peripheral CD11c^{+} macrophages. Furthermore, perineurally administered IL-4 can act on macrophages, which leads to a change in their state from pro- to anti-inflammatory via a STAT6-dependent mechanism [11] and further to a release of opioid peptides that are key factors in the suppression of neuropathic pain [10]. In the SDH, IGF1 appears to be necessary for the pain-relieving effect of CD11c^{+} microglia induced by IL-4. This is supported by data obtained from microglia-selective IGF1-knockout mice (*Cx3cr1*$^{CreERT2/+}$;*Igf1*$^{flox/flox}$ mice treated with tamoxifen). Although *Cx3cr1*$^{+}$ cells, other than CD11c^{+} microglia, also lack *Igf1* in these mice, given *Igf1* expression is much higher in CD11c^{+} microglia than in CD11c^{neg} microglia [18], IGF1 from CD11c^{+} microglia would play an important role in IL-4-induced pain remission. Thus, while IL-4

acts on macrophages and microglia in the DRG/injured nerves and the SDH, respectively, the molecular basis of its ameliorating effects on neuropathic pain hypersensitivity is different.

Another notable finding of this study was that the emergence of CD11c$^+$ spinal microglia following nerve injury was impaired in the SNI model, which did not exhibit spontaneous remission of behavioral pain hypersensitivity. This raises the possibility that the reduced ability of spinal microglia to shift toward the CD11c$^+$ state in the SNI model contributes, at least in part, to long-lasting pain hypersensitivity because SpNT mice with depleted CD11c$^+$ spinal microglia have been shown to exhibit persistent pain hypersensitivity [18]. Considering our finding that the total number of spinal microglia was comparable between the SpNT and SNI models, the signal(s) for microglia to transition to the CD11c$^+$ state, rather than to the initial activation after nerve injury, could be different in these models. The mechanisms underlying this difference require further investigation, but we highlight that even under such conditions, IL-4 administered intrathecally induces the appearance of CD11c$^+$ microglia in the SDH and exerts a pain-remitting effect in a manner that dependent on CD11c$^+$ microglia. These data suggest that spinal microglia in the SNI model retain the ability to respond to IL-4, allowing microglia to be in a CD11c$^+$ state that remits neuropathic pain and broadly extends their therapeutic potential to neuropathic pain.

In this study, we showed an ability of IL-4, known as a T-cell-derived factor, to increase CD11c$^+$ microglia and to control neuropathic pain. Recent studies have also indicated that immune cells such as CD8$^+$ T cells infiltrating into spinal cord [37], and

regulatory T cells [38,39] and MRC1^{+} macrophages [40] in the spinal meninges have important roles in controlling microglial states and neuropathic pain. Thus, these findings provide new insights into the mechanisms of the neuro-immune interactions that regulate neuropathic pain. Furthermore, our data, demonstrating that IL-4 increases CD11c^{+} microglia without affecting the total number of microglia, could open a new avenue for developing strategies to modulate microglial subpopulations through molecular targeting, which may lead to new analgesics. However, given IL-4's association with allergic responses, further investigation of the specific signaling pathways and molecular processes by which IL-4 induces a transition of spinal microglia to the CD11c^{+} state may provide clues to discovering new targets that offer more selective and safer therapeutic approaches. Moreover, since CD11c^{+} microglia have been implicated in other CNS diseases (e.g., Alzheimer disease [41], amyotrophic lateral sclerosis [42], and multiple sclerosis [43]), further investigations into the mechanisms driving CD11c^{+} microglia induction could provide insights into novel therapeutic strategies not only for neuropathic pain but also for other CNS diseases.

Acknowledgments: We would like to thank Editage for editing a draft of this manuscript. This work was supported by Japan Society for the Promotion of Science (JSPS) KAKENHI Grants JP19H05658 (M.T.), JP20H05900 (M.T.) and JP24H00067 (M.T.), by the Core Research for Evolutional Science and Technology (CREST) program from AMED under Grant Number 25gm1510013h (M.T.) by Research Support Project for Life Science and Drug Discovery (Basis for Supporting Innovative Drug Discovery and Life Science Research (BINDS)) from AMED under Grant Number

JP254ama121031 (M.T.). T.M. was supported by AMED (JP20gm6310016, JP21wm0425001, JP23gm1910004, JP23jf0126004, 24zf0127012), JSPS (KAKENHI JP21H02752, JP22H05062, JP25H01009), The Mitsubishi Foundation, Daiichi Sankyo Foundation of Life Science, Mochida Memorial Foundation for Medical and Pharmaceutical Research, Astellas Foundation for Research on Metabolic disorders, Ono Pharmaceutical Foundation for Oncology, Immunology and Neurology, The Nakajima Foundation, The Uehara Memorial Foundation and Takeda Science Foundation. K.K. was supported by JSPS (KAKENHI JP23K19403, JP24K18621), JST (ACT-X Grant Number JPMJAX232B), Chugai Foundation for Innovative Drug Discovery Science, and The Ichiro Kanehara Foundation. This work was supported in part by the MEXT Cooperative Research Project Program, Medical Research Center Initiative for High Depth Omics, and CURE:JPMXP1323015486 for MIB, Kyushu University.

Author Contributions: K.K. designed experiments, performed almost all experiments, analyzed the data, and wrote the manuscript. R.S. performed some experiments and analyzed the data. K.H. assisted some experiments. T.M. provided advice for some experiments. M.T. conceived this project, designed experiments, supervised the overall project, and wrote the manuscript. All of the authors read and discussed the manuscript.

Declaration of interests: The authors declare no competing interests.

Figure titles and legends

Figure 1. IL-4 increases CD11c^{+} microglia in the SDH and ameliorates pain hypersensitivity in the SpNT mice.

(*A*) Paw withdrawal threshold (PWT) of *Itgax-Venus* mice before (Pre) and after SpNT (n = 7–8 mice). IL-4 or PBS was intrathecally administrated from day 14 to day 16 post-SpNT (once a day for three days). ****P < 0.0001 versus the ipsilateral side of PBS-treated group, two-way ANOVA with post hoc Tukey multiple comparison test. (*B*) Venus fluorescence (yellow) and P2Y12R and IBA1 immunostaining (magenta and cyan, respectively) in the SDH of *Itgax-Venus* mice with SpNT 21 days after PBS or IL-4 treatment (from day 14 to 16). Scale bars, 200 µm (middle), 100 µm (right). (*C*) Colocalization of Venus, P2Y12R and IBA1. Scale bar, 20 µm. (*D*) Flow cytometric quantification for the number of $CD11c^+$ ($CD11b^+CD45^+Venus^+$) and total ($CD11b^+CD45^+$) microglia in the 3–4th lumbar SDH contralateral (*C*) and ipsilateral (I) to SpNT (n = 6–7 mice). One-way ANOVA with post hoc Tukey multiple comparison test. Data are shown as mean ± SEM.

Figure 1—figure supplement 1. Monocytes/macrophages in the SDH and DRG after intrathecal administration of IL-4.

Immunohistochemical analysis of the SDH (*A*) and the DRG (*B*) of naive WT mice and SpNT-WT mice with intrathecal injection of PBS or IL-4 (from day 14 to 16 post-SpNT). Immunofluorescence of CD169, CD11b, P2Y12R, and IBA1 in the SDH (L4) ipsilateral to the SpNT (day 17) (*A*) and of CCR2 and IBA1 in the DRG (L4) ipsilateral to the SpNT (day 17) (*B*). Scale bars, 100 µm (*A*) and 40 µm (*B*).

Figure 2. IL-4-induced remission of pain hypersensitivity requires spinal $CD11c^+$ microglia.

(*A*) Paw withdrawal threshold (PWT) of *Itgax-DTR-EGFP* mice before (Pre) and after SpNT (n = 6 –7 mice). IL-4 or PBS was intrathecally administrated from days 14 to 16 post-SpNT (once a day for three days). On day 17, DTX (0.5 ng/mouse) or PBS was intrathecally injected. ****P < 0.0001 versus the ipsilateral side of PBS-PBS group, ††††P < 0.0001 versus the ipsilateral side of IL-4-PBS group, two-way ANOVA with post hoc Tukey multiple comparison test. (*B*) Flow cytometric quantification for the number of CD11c^{+} microglia (CD11b^{+}CD45^{+}EGFP^{+}) in the 3–4th lumbar SDH contralateral (C) and ipsilateral (I) to SpNT in *Itgax-DTR-EGFP* mice treated with PBS/PBS, IL-4/PBS, or IL-4/DTX (n = 4–5 mice). One-way ANOVA with post hoc Tukey multiple comparison test. Data are shown as mean ± SEM.

Figure 3. IL-4 alleviates pain hypersensitivity in female mice.

Paw withdrawal threshold (PWT) of *Itgax-DTR-EGFP* mice before (Pre) and after SpNT (n = 6 female mice). IL-4 or PBS was intrathecally administrated from days 14 to 16 post-SpNT (once a day for three days). On day 17, DTX (0.5 ng/mouse) or PBS was intrathecally injected. ****P < 0.0001 versus the ipsilateral side of PBS-PBS group, †††P < 0.001 versus the ipsilateral side of IL-4-PBS group, two-way ANOVA with post hoc Tukey multiple comparison test. Data are shown as mean ± SEM.

Figure 4. CD11c^{+} cells in the DRG are involved in IL-4-induced remission of pain hypersensitivity.

(*A* and *B*) Immunohistochemical analyses of CD11c^{+} cells (EGFP^{+} IBA1^{+}) in the DRG (*A*) and SDH (*B*) on day 18 post-SpNT of *Itgax-DTR-EGFP* mice treated intrathecally with

IL-4 (from day 14 to 16) (n = 4–5 mice). DTX (2 ng/g) or PBS was intraperitoneally injected on day 17. The myeloid marker IBA1 was also stained in the SDH (*B*). Scale bars, 100 µm. Unpaired t-test. (*C*) Effect of DTX (2 ng/g) intraperitoneally injected (on day 17) on PWT of SpNT mice treated intrathecally with PBS or IL-4 (from day 14 to 16) (n = 5 mice). Data are shown as mean ± SEM.

Figure 5. Blunted appearance of CD11c^{+} microglia in the SDH after SNI.

(*A*) PWT of wild-type (WT) mice before (Pre) and after SpNT and SNI (n = 5 mice). (*B*) Venus (yellow) and IBA1 immunostaining (magenta) in the SDH of SpNT and SNI mice on day 14. Scale bar, 200 µm. (*C*) Flow cytometric quantification of the number of CD11c^{+} (CD11b^{+}CD45^{+}Venus^{+}) and total (CD11b^{+}CD45^{+}) microglia in the 3–4th lumbar SDH of *Itgax-Venus* mice after SpNT and SNI (n = 3–5 mice). ****P < 0.0001 versus the ipsilateral side of SNI group, two-way ANOVA with post hoc Tukey multiple comparison test. Data are shown as mean ± SEM.

Figure 6. Expression of Igf1 is lower in the SNI model.

(*A*-*C*) *Igf1* mRNA in total RNA extracted from sorted SDH microglia (*A*; n = 4 mice), from tissue homogenate of the upper half of the SDH (*B*; n = 3–4 mice), or from the sorted CD11c^{high} microglia (*C*; n = 5–6 mice) in *Itgax-Venus* mice was quantified by qPCR on day 36 post-SpNT or SNI. Cells and tissues were collected from the contralateral (C) and ipsilateral (I) side to the SpNT or SNI. Values represent the relative ratio of *Igf1* mRNA (normalized to the value for *Actb* mRNA) to the ipsilateral (*A* and *C*) or contralateral (*B*) side of SpNT mice. One-way ANOVA with post hoc Tukey multiple

comparison test (*A* and *B*). Unpaired t-test (*C*). Data are shown as mean ± SEM.

Figure 7. IL-4 increases CD11c$^+$ microglia in the SDH and ameliorates pain hypersensitivity in the SNI mice.

(*A*) Venus fluorescence (yellow) and P2Y12R and IBA1 immunostaining (magenta and cyan, respectively) in the SDH of *Itgax-Venus* mice with SpNT after PBS or IL-4 treatment. Scale bar, 200 µm. (*B*) Colocalization of Venus, P2Y12R and IBA1. Scale bar, 20 µm. (*C*) Flow cytometric quantification for the number of CD11c$^+$ (CD11b$^+$CD45$^+$Venus$^+$) and total (CD11b$^+$CD45$^+$) microglia in the 3–4th lumbar SDH contralateral (C) and ipsilateral (I) to SNI (n = 7 mice). One-way ANOVA with post hoc Tukey multiple comparison test. (*D*) Paw withdrawal threshold (PWT) of *Itgax-Venus* mice before (Pre) and after SNI (n = 6–8 mice). IL-4 or PBS was intrathecally administrated from day 14 to 16 post-SNI (once a day for three days). *P < 0.05, ***P < 0.001 versus the ipsilateral side of PBS group, two-way ANOVA with post hoc Tukey multiple comparison test. Data are shown as mean ± SEM.

Figure 8. IL-4 alleviates SNI-induced pain hypersensitivity in CD11c$^+$ microglia- and IGF1- dependent manners.

(*A*) Flow cytometric quantification for the number of CD11c$^+$ microglia (CD11b$^+$CD45$^+$EGFP$^+$) in the 3–4th lumbar SDH contralateral (*C*) and ipsilateral (I) to SNI in *Itgax-DTR-EGFP* mice treated with IL-4/PBS or IL-4/DTX (n = 6 mice). One-way ANOVA with post hoc Tukey multiple comparison test. (*B*) PWT of *Itgax-DTR-EGFP*

mice before (Pre) and after SNI (n = 6 mice). IL-4 was intrathecally administrated from day 14 to 16 post-SNI (once a day for three days). On day 17, DTX (0.5 ng/mouse) or PBS was intrathecally injected. **P < 0.01 versus the ipsilateral side of IL-4-PBS group, two-way ANOVA with post hoc Tukey multiple comparison test. (C) PWT of *Cx3cr1*$^{CreERT2/+}$;*Igf1*$^{flox/flox}$ mice before (Pre) and after SNI (n = 5–7 mice). Tamoxifen or vehicle were administered 4 weeks before SNI to induce recombination. IL-4 was intrathecally administrated from day 14 to 16 post-SNI (once a day for three days). ***P < 0.001 versus the ipsilateral side of Corn oil group, two-way ANOVA with post hoc Tukey multiple comparison test. Data are shown as mean ± SEM.

Materials and Methods

Key Resources Table

Reagent type (species) or resource	Designation	Source or reference	Identifiers	Additional information
strain, strain background (include species and sex here)	C57BL/6J	The Jackson Laboratory Japan	NA	
genetic reagent (include species here)	B6.Cg-Tg(Itgax-Venus)Mnz/J	Jackson Laboratory	RRID:IMSR_JAX:008829	

genetic reagent (include species here)	B6.FVB-1700016L21RikTg(Itgax-DTR/EGFP)57Lan/J	Jackson Laboratory	RRID:IMSR_JAX:004509	
genetic reagent (include species here)	B6.129P2(Cg)-Cx3cr1tm2.1(cre/ERT2)Litt/WganJ	Jackson Laboratory	RRID:IMSR_JAX:021160	
genetic reagent (include species here)	B6.129(FVB)-Igf1tm1Dlr/J	Jackson Laboratory	RRID:IMSR_JAX:016831	
antibody	Guinea pig anti-IBA1	Synaptic Systems	RRID:AB_2924932	1:2000
antibody	Rabbit anti-P2Y12R	AnaSpec	RRID:AB_2298886	1:2000
antibody	Rabbit anti-GFP	MBL International	RRID:AB_591819	1:1000
antibody	APC anti-mouse CD169	Biolegend	RRID:AB_2565640	1:500
antibody	Rabbit anti-CCR2	Abcam	RRID:AB_2893307	1:500
antibody	Goat Anti-Guinea pig IgG H&L (Alexa Fluor® 405)	Abcam	RRID:AB_2827755	1:1000
antibody	Goat anti-Rabbit IgG (H+L) Highly Cross-Adsorbed Secondary Antibody, Alexa Fluor™ 488	Thermo Fisher Scientific	RRID:AB_2576217	1:1000
antibody	Goat anti-Rabbit IgG (H+L) Highly Cross-Adsorbed Secondary Antibody, Alexa Fluor™ 546	Thermo Fisher Scientific	RRID:AB_2534093	1:1000
antibody	Rat Anti-CD16 / CD32 Monoclonal Antibody, Unconjugated, Clone 2.4G2	BD Biosciences	RRID:AB_394657	1:200

antibody	Rat Anti-CD11b Monoclonal Antibody, Alexa Fluor™ 647 Conjugated, Clone M1/70	BD Biosciences	RRID:AB_396796	1:1000
antibody	PE anti-mouse CD45	BioLegend	RRID:AB_312971	1:1000
antibody	Brilliant Violet 785(TM) anti-mouse/human CD11b	BioLegend	RRID:AB_2561373	1:1000
antibody	APC anti-mouse CD206 (MMR)	BioLegend	RRID:AB_10900231	1:200
peptide, recombinant protein	Recombinant Murine IL-4	PeproTech	214-14	
commercial assay or kit	Myelin Removal Beads II	Miltenyi Biotec	130-096-433	
commercial assay or kit	MACS LS column	Miltenyi Biotec	130-042-401	
commercial assay or kit	Quick-RNA Micro-Prep kit	ZYMO	R1051	
commercial assay or kit	Trisure	Bioline	BIO-38032	
commercial assay or kit	Prime Script reverse transcriptase	Takara	2680B	
commercial assay or kit	Premix Ex Taq™ (Probe qPCR)	Takara	RR390B	
chemical compound, drug	tamoxifen	SIGMA	T5648	
chemical compound, drug	Diphtheria Toxin Solution	Wako	048-34371	
chemical compound, drug	collagenase D	Roche	11088866001	
chemical compound, drug	dispase	GIBCO	17105041	

chemical compound, drug	RNAlater	Invitrogen	AM7021	
chemical compound, drug	7-aminoactinomycin D	Miltenyi Biotec	170-081-088	
software, algorithm	LSM700 Imaging System	Carl Zeiss	NA	
software, algorithm	CytoFLEX SRT	Beckman Coulter	NA	
software, algorithm	FlowJo	BD	RRID:SCR_008520	
software, algorithm	FACSAria III	BD Biosciences	NA	
software, algorithm	QuantStudio® 3	Applied Biosystems	NA	
software, algorithm	Prism 7	GraphPad	NA	

Mice. C57BL/6 mice were purchased from Charles River Japan (Kanagawa, Japan). *Itgax-Venus* mice (B6.Cg-Tg(*Itgax-Venus*)Mnz/J) [21], *Itgax-DTR-EGFP* mice (B6.FVB-1700016L21Rik$^{Tg(Itgax\text{-}DTR/EGFP)57Lan/J}$) [24], *Cx3cr1*$^{CreERT2/+}$ mice (B6.129P2(Cg)-*Cx3cr1*$^{tm2.1(cre/ERT2)Litt}$/WganJ) [26], *Igf1*$^{flox/flox}$ mice (B6.129(FVB)-*Igf1*^{tm1Dlr}/J) [44] were purchased from Jackson Laboratory (Bar Harbor, ME). The data were obtained from male mice except for the data shown in Figures 1D, 3, and 7C. For induction of Cre recombinase, *Cx3cr1*$^{CreERT2/+}$; *Igf1*$^{flox/flox}$ mice were injected subcutaneously with 4 mg of tamoxifen (Sigma, St. Louis, MO) dissolved in 200 μL corn oil (Wako, Osaka, Japan) twice with a 48-hr interval. Four weeks later when gene-deleting CX3CR1^{+} cells in peripheral tissues including the DRG has been shown to be replaced by non-deleting

cells [26,45], the mice were subjected to nerve injury. All mice used were aged 5–14 weeks at the start of each experiment, and were housed individually or in groups at a temperature of 22±1°C with a 12-hr light–dark cycle, and were fed food and water ad libitum. All animal experiments were conducted according to relevant national and international guidelines contained in the 'Act on Welfare and Management of Animals' (Ministry of Environment of Japan) and 'Regulation of Laboratory Animals' (Kyushu University) and under the protocols approved by the Institutional Animal Care and Use committee review panels at Kyushu University.

Peripheral nerve injury. We used two injury models, spinal nerve transection (SpNT) [18,46], which is a modified spinal nerve injury model [19], and spared nerve injury (SNI) [25]. For the SpNT model, under isoflurane (2%) anesthesia, a small incision at L3–S1 was made. The paraspinal muscle and fat were removed from the L5 traverse process, which exposed the parallel-lying L3 and L4 spinal nerves. The L4 nerve was then carefully isolated and cut while leaving the L3 spinal nerve intact. The wound and the surrounding skin were sutured with 5-0 silk. For the SNI model, according to a previously reported method [47], under isoflurane (2%) anesthesia, the skin on the left thigh was open, and terminal branches of the sciatic nerve were exposed by separating the thigh muscle layer using scissors and blunt forceps. Two of the three branches, the tibial and common peroneal nerves, were tightly ligated with 7-0 Nylon (NM-01, WASHIESU MEDICAL) and a small portion of the nerves distal to the ligation were removed while leaving the sural nerve intact. The wound and the surrounding skin were sutured with 5-0 silk.

Immunohistochemistry. According to our previously reported method [18], mice were

deeply anesthetized by i.p. injection of pentobarbital and perfused transcardially with phosphate buffered saline (PBS) followed by ice-cold 4% paraformaldehyde/PBS. Transverse L4 spinal cord sections (30 μm) or L4 dorsal root ganglion (DRG) sections (20 μm) were incubated for 48 hrs at 4 °C with primary antibody for IBA1 (1:2000; Cat# 234 308, Synaptic Systems), P2Y12R (1:2000; Cat# AS-55043A, AnaSpec), CCR2 (1:500; Cat# ab273050, Abcam), APC-conjugated CD169 (1:500, Cat# 142417, Biolegend), PE-conjugated CD11b (1:1000, Cat# 101207, Biolegend) or GFP (1:1000; Cat# 598, MBL Life science). Tissue sections were incubated with secondary antibodies conjugated to Alexa Fluor 405 (1:1000, Abcam), 488, or 546 (1:1000, Molecular Probes) and mounted with Vectashield. Three to five sections from one tissue were randomly selected and analyzed using an LSM700 Imaging System (Carl Zeiss, Japan).

Behavioral test. To assess mechanical sensitivity, calibrated von Frey filaments (0.02–2.0 g, North Coast Medical, USA) were applied to the plantar surfaces of the hindpaws of mice with or without PNI [18] and the 50% PWT was determined using the up–down method [48].

Intrathecal injection. Under 2% isoflurane anesthesia, a 30G needle attached to a 25-μL Hamilton syringe was inserted into the intervertebral space between L5 and L6 spinal vertebrae in mice, as previously described [18,49]. Recombinant Murine IL-4 was purchased from Peprotech (Cat# 214-14). IL-4 (40 ng/μL in PBS, 5 μL/mouse) or PBS as a control were intrathecally injected once a day for 3 days from day 14 post-PNI. DTX was purchased from Wako (Cat# 048-34371) and was injected intrathecally (0.1 ng/μL in PBS, 5 μL/mouse) or intraperitoneally (2 ng/g mouse) into *Itgax-DTR-EGFP* mice. Only

mice whose hypersensitivity was attenuated by IL-4 treatment were used for the DTX-induced cell depletion experiment shown in Figure 4C (10 out of 12 mice were included) and Figure 8B (12 out of 15 mice were included).

Flow cytometry. As previously described [18], mice were deeply anesthetized by i.p. injection of pentobarbital and perfused transcardially with PBS to remove the circulating blood from the vasculature. The spinal cord was rapidly and carefully removed from the vertebral column and placed into ice-cold Hanks' balanced salt solution (HBSS). The 3th–4th lumbar (L3/4) segments (2 mm long) of the spinal dorsal horn (SDH) ipsilateral and contralateral to nerve injury were separated. Unilateral spinal tissue pieces were treated with pre-warmed 0.8-mL enzymatic solution [0.2 U/mL collagenase D (Cat# 11088866001; Roche) and 4.3 U/mL dispase (Cat# 17105041; GIBCO)] in HBSS containing 2% fetal bovine serum (FBS) for 30 min at 37 °C. The tissues were homogenized by passing through a 23G needle attached with a 1-mL syringe and were further incubated for 15 min at 37 °C. After that, the tissues were homogenized by passing twice through a 26G needle, and the enzymatic reaction was stopped by adding EDTA (0.5 M). To count the number of $CD11c^+$ ($Venus^+$ or $EGFP^+$) microglia, cell suspension was blocked by incubating with Fc Block (Cat# 553142; BD Biosciences) for 5 min at 4 °C and immunostained with CD11b-AlexaFluor 647 (M1/70; 1:1000; Cat# 557686, BD Biosciences) and CD45-PE (1:1000; Cat# 103106, Biolegend) for 30 min at 4 °C in the dark. After washing, the pellet was resuspended in ice-cold HBSS-FBS and filtered through a 35-μm nylon cell strainer (BD Biosciences) to isolate tissue debris from the cell suspension. The total number of microglia ($CD11b^+$ $CD45^+$ cells) in the L3/4 spinal cord or SDH was analyzed using CytoFLEX SRT (Beckman Coulter) and FlowJo

software (TreeStar). Microglia with Venus fluorescence higher in intensity than that observed in microglia of wild-type mice were analyzed as $CD11c^{+}$ microglia.

Fluorescent activated cell sorting (FACS). Spinal tissues were removed and homogenized as described above. Myelin debris was removed from the cell suspension using Myelin Removal Beads II and a MACS LS column (Miltenyi Biotec, Bergisch-Gladbach, Germany) according to the manufacturer's protocol and our previously reported method [18]. After centrifugation (300 × g, 10 min, 4 °C), the cells were resuspended in HBSS containing 10% FBS. The cell suspension was blocked by incubating with Fc Block and immunostained with CD11b-Brilliant Violet 785 (1:1000; Cat# 101243, BioLegend), CD206-APC (1:200; Cat# 141708, BioLegend), and CD45-PE (1:1000; Cat# 103105, BioLegend) for 30 min at 4 °C in the dark. After washing, cell suspension was treated with 7-aminoactinomycin D (7-AAD; Miltenyi Biotec) and incubate for 10 min on ice for viability staining prior to cell sorting. $CD11b^{+}$ $CD45^{+}$ $CD206^{neg}$ $7\text{-}AAD^{neg}$-singlet cells are gated as live microglia and sorted using FACSAria III (BD Biosciences) or CytoFLEX SRT. The sorted cells were directly collected in lysis buffer for total RNA extraction using the Quick-RNA Micro-Prep kit (ZYMO). $CD11c^{high}$ microglia were collected as cells with Venus fluorescence higher than the median Venus fluorescence of all $CD11c^{+}$ microglia [18]

mRNA extraction from spinal cord homogenates. Mice were deeply anesthetized by pentobarbital and perfused transcardially with ice-cold PBS followed by RNAlater™ Stabilization Solution (Cat# AM7021, Invitrogen). The isolated SDH tissue around the boundary between L3 and L4 segments was isolated and separated into the ipsilateral

and contralateral sides, and the upper half portion of the SDH of each side was dissected as described previously [18]. Total RNA was extracted from tissue homogenates using Trisure (CAT# BIO-38032, Bioline, USA) according to manufacturer's protocol and purified with the Quick-RNA Micro-Prep kit (ZYMO).

qPCR. As described previously [18], the extracted RNA from the sorted cells or the tissue was transferred to reverse transcriptional reaction with Prime Script reverse transcriptase (2680B, Takara, Japan). Quantitative PCR (qPCR) was performed with Premix Ex Taq™ (Cat# RR390B, Takara, Japan) using QuantStudio® 3 (Applied Biosystems, USA). Expression levels were normalized to the values for *Actb*. The sequences of TaqMan primer pairs and probe are described below: *Actb*: 5'-FAM-CCTGGCCTCACTGTCCACCTTCCA-TAMRA-3' (probe), 5'-CCTGAGCGCAAGTACTCTGTGT-3' (forward primer), 5'-CTGCTTGCTGATCCACATCTG-3' (reverse primer); *Igf1*: 5'- /56-FAM/TCCGGAAGC/ZEN/AACACTCACATCCACAA/3IABkFQ/-3' (probe), 5'-AGTACATCTCCAGTCTCCTCA-3' (forward primer), 5'- ATGCTCTTCAGTTCGTGTGT-3' (reverse primer).

Quantification and statistical analysis. All data are shown as mean ± s.e.m. Statistical significance was determined using the unpaired t-test, two-way ANOVA with post hoc Tukey's multiple comparison test or one-way ANOVA with post hoc Tukey's multiple comparison test using GraphPad Prism 7 software. Differences were considered significant at $P<0.05$.

References

1. Colloca, L., Ludman, T., Bouhassira, D., Baron, R., Dickenson, A.H., Yarnitsky, D., Freeman, R., Truini, A., Attal, N., Finnerup, N.B., et al. (2017). Neuropathic pain. Nat Rev Dis Primers *3*, 17002. https://doi.org/10.1038/nrdp.2017.2.
2. Finnerup, N.B., Kuner, R., and Jensen, T.S. (2021). Neuropathic pain: From mechanisms to treatment. Physiol. Rev. *101*, 259–301. https://doi.org/10.1152/physrev.00045.2019.
3. Ji, R.-R., Chamessian, A., and Zhang, Y.-Q. (2016). Pain regulation by non-neuronal cells and inflammation. Science *354*, 572–577. https://doi.org/10.1126/science.aaf8924.
4. Inoue, K., and Tsuda, M. (2018). Microglia in neuropathic pain: cellular and molecular mechanisms and therapeutic potential. Nat. Rev. Neurosci. *19*, 138–152. https://doi.org/10.1038/nrn.2018.2.
5. Ji, R.-R., Donnelly, C.R., and Nedergaard, M. (2019). Astrocytes in chronic pain and itch. Nat. Rev. Neurosci. *20*, 667–685. https://doi.org/10.1038/s41583-019-0218-1.
6. Grace, P.M., Hutchinson, M.R., Maier, S.F., and Watkins, L.R. (2014). Pathological pain and the neuroimmune interface. Nat. Rev. Immunol. *14*, 217–231. https://doi.org/10.1038/nri3621.
7. Vanderwall, A.G., and Milligan, E.D. (2019). Cytokines in Pain: Harnessing Endogenous Anti-Inflammatory Signaling for Improved Pain Management. Front. Immunol. *10*, 3009. https://doi.org/10.3389/fimmu.2019.03009.
8. Cunha, F.Q., Poole, S., Lorenzetti, B.B., Veiga, F.H., and Ferreira, S.H. (1999). Cytokine-mediated inflammatory hyperalgesia limited by interleukin-4. Br. J.

Pharmacol. *126*, 45–50. https://doi.org/10.1038/sj.bjp.0702266.

9. Vale, M.L., Marques, J.B., Moreira, C.A., Rocha, F.A.C., Ferreira, S.H., Poole, S., Cunha, F.Q., and Ribeiro, R.A. (2003). Antinociceptive effects of interleukin-4, -10, and -13 on the writhing response in mice and zymosan-induced knee joint incapacitation in rats. J. Pharmacol. Exp. Ther. *304*, 102–108. https://doi.org/10.1124/jpet.102.038703.

10. Celik, M.Ö., Labuz, D., Keye, J., Glauben, R., and Machelska, H. (2020). IL-4 induces M2 macrophages to produce sustained analgesia via opioids. JCI Insight *5*. https://doi.org/10.1172/jci.insight.133093.

11. Kiguchi, N., Kobayashi, Y., Saika, F., Sakaguchi, H., Maeda, T., and Kishioka, S. (2015). Peripheral interleukin-4 ameliorates inflammatory macrophage-dependent neuropathic pain. Pain *156*, 684–693. https://doi.org/10.1097/j.pain.0000000000000097.

12. Labuz, D., Celik, M.Ö., Seitz, V., and Machelska, H. (2021). Interleukin-4 Induces the Release of Opioid Peptides from M1 Macrophages in Pathological Pain. J. Neurosci. *41*, 2870–2882. https://doi.org/10.1523/JNEUROSCI.3040-20.2021.

13. Nie, B., Liu, C., Bai, X., Chen, X., Wu, S., Zhang, S., Huang, Z., Xie, M., Xu, T., Xin, W., et al. (2018). AKAP150 involved in paclitaxel-induced neuropathic pain via inhibiting CN/NFAT2 pathway and downregulating IL-4. Brain Behav. Immun. *68*, 158–168. https://doi.org/10.1016/j.bbi.2017.10.015.

14. Okutani, H., Yamanaka, H., Kobayashi, K., Okubo, M., and Noguchi, K. (2018). Recombinant interleukin-4 alleviates mechanical allodynia via injury-induced interleukin-4 receptor alpha in spinal microglia in a rat model of neuropathic pain.

Glia *66*, 1775–1787. https://doi.org/10.1002/glia.23340.

15. Hao, S., Mata, M., Glorioso, J.C., and Fink, D.J. (2006). HSV-mediated expression of interleukin-4 in dorsal root ganglion neurons reduces neuropathic pain. Mol. Pain *2*, 6. https://doi.org/10.1186/1744-8069-2-6.
16. Kohno, K., Kitano, J., Kohro, Y., Tozaki-Saitoh, H., Inoue, K., and Tsuda, M. (2018). Temporal Kinetics of Microgliosis in the Spinal Dorsal Horn after Peripheral Nerve Injury in Rodents. Biol. Pharm. Bull. *41*, 1096–1102. https://doi.org/10.1248/bpb.b18-00278.
17. Tansley, S., Uttam, S., Ureña Guzmán, A., Yaqubi, M., Pacis, A., Parisien, M., Deamond, H., Wong, C., Rabau, O., Brown, N., et al. (2022). Single-cell RNA sequencing reveals time- and sex-specific responses of mouse spinal cord microglia to peripheral nerve injury and links ApoE to chronic pain. Nat. Commun. *13*, 843. https://doi.org/10.1038/s41467-022-28473-8.
18. Kohno, K., Shirasaka, R., Yoshihara, K., Mikuriya, S., Tanaka, K., Takanami, K., Inoue, K., Sakamoto, H., Ohkawa, Y., Masuda, T., et al. (2022). A spinal microglia population involved in remitting and relapsing neuropathic pain. Science *376*, 86–90. https://doi.org/10.1126/science.abf6805.
19. Ho Kim, S., and Mo Chung, J. (1992). An experimental model for peripheral neuropathy produced by segmental spinal nerve ligation in the rat. Pain *50*, 355–363. https://doi.org/10.1016/0304-3959(92)90041-9.
20. Rigaud, M., Gemes, G., Barabas, M.-E., Chernoff, D.I., Abram, S.E., Stucky, C.L., and Hogan, Q.H. (2008). Species and strain differences in rodent sciatic nerve anatomy: implications for studies of neuropathic pain. Pain *136*, 188–201.

https://doi.org/10.1016/j.pain.2008.01.016.

21. Lindquist, R.L., Shakhar, G., Dudziak, D., Wardemann, H., Eisenreich, T., Dustin, M.L., and Nussenzweig, M.C. (2004). Visualizing dendritic cell networks in vivo. Nat. Immunol. *5*, 1243–1250. https://doi.org/10.1038/ni1139.

22. Butovsky, O., Jedrychowski, M.P., Moore, C.S., Cialic, R., Lanser, A.J., Gabriely, G., Koeglsperger, T., Dake, B., Wu, P.M., Doykan, C.E., et al. (2014). Identification of a unique TGF-β-dependent molecular and functional signature in microglia. Nat. Neurosci. *17*, 131–143. https://doi.org/10.1038/nn.3599.

23. Ito, D., Imai, Y., Ohsawa, K., Nakajima, K., Fukuuchi, Y., and Kohsaka, S. (1998). Microglia-specific localisation of a novel calcium binding protein, Iba1. Brain Res. Mol. Brain Res. *57*, 1–9. https://doi.org/10.1016/s0169-328x(98)00040-0.

24. Jung, S., Unutmaz, D., Wong, P., Sano, G.-I., De los Santos, K., Sparwasser, T., Wu, S., Vuthoori, S., Ko, K., Zavala, F., et al. (2002). In vivo depletion of CD11c+ dendritic cells abrogates priming of CD8+ T cells by exogenous cell-associated antigens. Immunity *17*, 211–220. https://doi.org/10.1016/s1074-7613(02)00365-5.

25. Decosterd, I., and Woolf, C.J. (2000). Spared nerve injury: an animal model of persistent peripheral neuropathic pain. Pain *87*, 149–158. https://doi.org/10.1016/S0304-3959(00)00276-1.

26. Parkhurst, C.N., Yang, G., Ninan, I., Savas, J.N., Yates, J.R., 3rd, Lafaille, J.J., Hempstead, B.L., Littman, D.R., and Gan, W.-B. (2013). Microglia promote learning-dependent synapse formation through brain-derived neurotrophic factor. Cell *155*, 1596–1609. https://doi.org/10.1016/j.cell.2013.11.030.

27. Shibata, Y., Matsumoto, Y., Kohno, K., Nakashima, Y., and Tsuda, M. (2025).

Microgliosis in the spinal dorsal horn early after peripheral nerve injury is associated with damage to primary afferent Aβ-fibers. Cells *14*, 666. https://doi.org/10.3390/cells14090666.

28. Masuda, T., Tsuda, M., Yoshinaga, R., Tozaki-Saitoh, H., Ozato, K., Tamura, T., and Inoue, K. (2012). IRF8 is a critical transcription factor for transforming microglia into a reactive phenotype. Cell Rep. *1*, 334–340. https://doi.org/10.1016/j.celrep.2012.02.014.

29. Masuda, T., Iwamoto, S., Yoshinaga, R., Tozaki-Saitoh, H., Nishiyama, A., Mak, T.W., Tamura, T., Tsuda, M., and Inoue, K. (2014). Transcription factor IRF5 drives P2X4R+-reactive microglia gating neuropathic pain. Nat. Commun. *5*, 3771. https://doi.org/10.1038/ncomms4771.

30. Tsuda, M., Shigemoto-Mogami, Y., Koizumi, S., Mizokoshi, A., Kohsaka, S., Salter, M.W., and Inoue, K. (2003). P2X4 receptors induced in spinal microglia gate tactile allodynia after nerve injury. Nature *424*, 778–783. https://doi.org/10.1038/nature01786.

31. Coull, J.A.M., Beggs, S., Boudreau, D., Boivin, D., Tsuda, M., Inoue, K., Gravel, C., Salter, M.W., and De Koninck, Y. (2005). BDNF from microglia causes the shift in neuronal anion gradient underlying neuropathic pain. Nature *438*, 1017–1021. https://doi.org/10.1038/nature04223.

32. Sideris-Lampretsas, G., and Malcangio, M. (2022). Pain-resolving microglia. Science *376*, 33–34. https://doi.org/10.1126/science.abo5592.

33. Tsuda, M., Masuda, T., and Kohno, K. (2023). Microglial diversity in neuropathic pain. Trends Neurosci. *46*, 597–610. https://doi.org/10.1016/j.tins.2023.05.001.

34. Butovsky, O., Koronyo-Hamaoui, M., Kunis, G., Ophir, E., Landa, G., Cohen, H., and Schwartz, M. (2006). Glatiramer acetate fights against Alzheimer's disease by inducing dendritic-like microglia expressing insulin-like growth factor 1. Proceedings of the National Academy of Sciences *103*, 11784–11789. https://doi.org/10.1073/pnas.0604681103.

35. Chiu, I.M., Chen, A., Zheng, Y., Kosaras, B., Tsiftsoglou, S.A., Vartanian, T.K., Brown, R.H., Jr, and Carroll, M.C. (2008). T lymphocytes potentiate endogenous neuroprotective inflammation in a mouse model of ALS. Proc. Natl. Acad. Sci. U. S. A. *105*, 17913–17918. https://doi.org/10.1073/pnas.0804610105.

36. Butovsky, O., Talpalar, A.E., Ben-Yaakov, K., and Schwartz, M. (2005). Activation of microglia by aggregated β-amyloid or lipopolysaccharide impairs MHC-II expression and renders them cytotoxic whereas IFN-γ and IL-4 render them protective. Mol. Cell. Neurosci. *29*, 381–393. https://doi.org/10.1016/j.mcn.2005.03.005.

37. Fan, C.Y., McAllister, B.B., Stokes-Heck, S., Harding, E.K., Pereira de Vasconcelos, A., Mah, L.K., Lima, L.V., van den Hoogen, N.J., Rosen, S.F., Ham, B., et al. (2025). Divergent sex-specific pannexin-1 mechanisms in microglia and T cells underlie neuropathic pain. Neuron *113*, 896-911.e9. https://doi.org/10.1016/j.neuron.2025.01.005.

38. Kuhn, J.A., Vainchtein, I.D., Braz, J., Hamel, K., Bernstein, M., Craik, V., Dahlgren, M.W., Ortiz-Carpena, J., Molofsky, A.B., Molofsky, A.V., et al. (2021). Regulatory T-cells inhibit microglia-induced pain hypersensitivity in female mice. Elife *10*. https://doi.org/10.7554/eLife.69056.

39. Midavaine, É., Moraes, B.C., Benitez, J., Rodriguez, S.R., Braz, J.M., Kochhar,

N.P., Eckalbar, W.L., Tian, L., Domingos, A.I., Pintar, J.E., et al. (2025). Meningeal regulatory T cells inhibit nociception in female mice. Science *388*, 96–104. https://doi.org/10.1126/science.adq6531.

40. Niehaus, J.K., Taylor-Blake, B., Loo, L., Simon, J.M., and Zylka, M.J. (2021). Spinal macrophages resolve nociceptive hypersensitivity after peripheral injury. Neuron *109*, 1274-1282.e6. https://doi.org/10.1016/j.neuron.2021.02.018.
41. Keren-Shaul, H., Spinrad, A., Weiner, A., Matcovitch-Natan, O., Dvir-Szternfeld, R., Ulland, T.K., David, E., Baruch, K., Lara-Astaiso, D., Toth, B., et al. (2017). A unique microglia type associated with restricting development of Alzheimer's disease. Cell *169*, 1276-1290.e17. https://doi.org/10.1016/j.cell.2017.05.018.
42. Xie, M., Liu, Y.U., Zhao, S., Zhang, L., Bosco, D.B., Pang, Y.-P., Zhong, J., Sheth, U., Martens, Y.A., Zhao, N., et al. (2022). TREM2 interacts with TDP-43 and mediates microglial neuroprotection against TDP-43-related neurodegeneration. Nat. Neurosci. *25*, 26–38. https://doi.org/10.1038/s41593-021-00975-6.
43. Wlodarczyk, A., Benmamar-Badel, A., Cédile, O., Jensen, K.N., Kramer, I., Elsborg, N.B., and Owens, T. (2018). CSF1R stimulation promotes increased neuroprotection by CD11c+ microglia in EAE. Front. Cell. Neurosci. *12*, 523. https://doi.org/10.3389/fncel.2018.00523.
44. Liu, J.L., Grinberg, A., Westphal, H., Sauer, B., Accili, D., Karas, M., and LeRoith, D. (1998). Insulin-like growth factor-I affects perinatal lethality and postnatal development in a gene dosage-dependent manner: manipulation using the Cre/loxP system in transgenic mice. Mol. Endocrinol. *12*, 1452–1462. https://doi.org/10.1210/mend.12.9.0162.

45. Peng, J., Gu, N., Zhou, L., B Eyo, U., Murugan, M., Gan, W.-B., and Wu, L.-J. (2016). Microglia and monocytes synergistically promote the transition from acute to chronic pain after nerve injury. Nat. Commun. *7*, 12029. https://doi.org/10.1038/ncomms12029.
46. Masuda, T., Kohro, Y., Inoue, K., and Tsuda, M. (2017). Peripheral Nerve Injury: a Mouse Model of Neuropathic Pain. Bio Protoc *7*, e2252. https://doi.org/10.21769/BioProtoc.2252.
47. Cichon, J., Sun, L., and Yang, G. (2018). Spared Nerve Injury Model of Neuropathic Pain in Mice. Bio Protoc *8*. https://doi.org/10.21769/bioprotoc.2777.
48. Chaplan, S.R., Bach, F.W., Pogrel, J.W., Chung, J.M., and Yaksh, T.L. (1994). Quantitative assessment of tactile allodynia in the rat paw. J. Neurosci. Methods *53*, 55–63. https://doi.org/10.1016/0165-0270(94)90144-9.
49. Hylden, J.L., and Wilcox, G.L. (1980). Intrathecal morphine in mice: a new technique. Eur. J. Pharmacol. *67*, 313–316. https://doi.org/10.1016/0014-2999(80)90515-4.

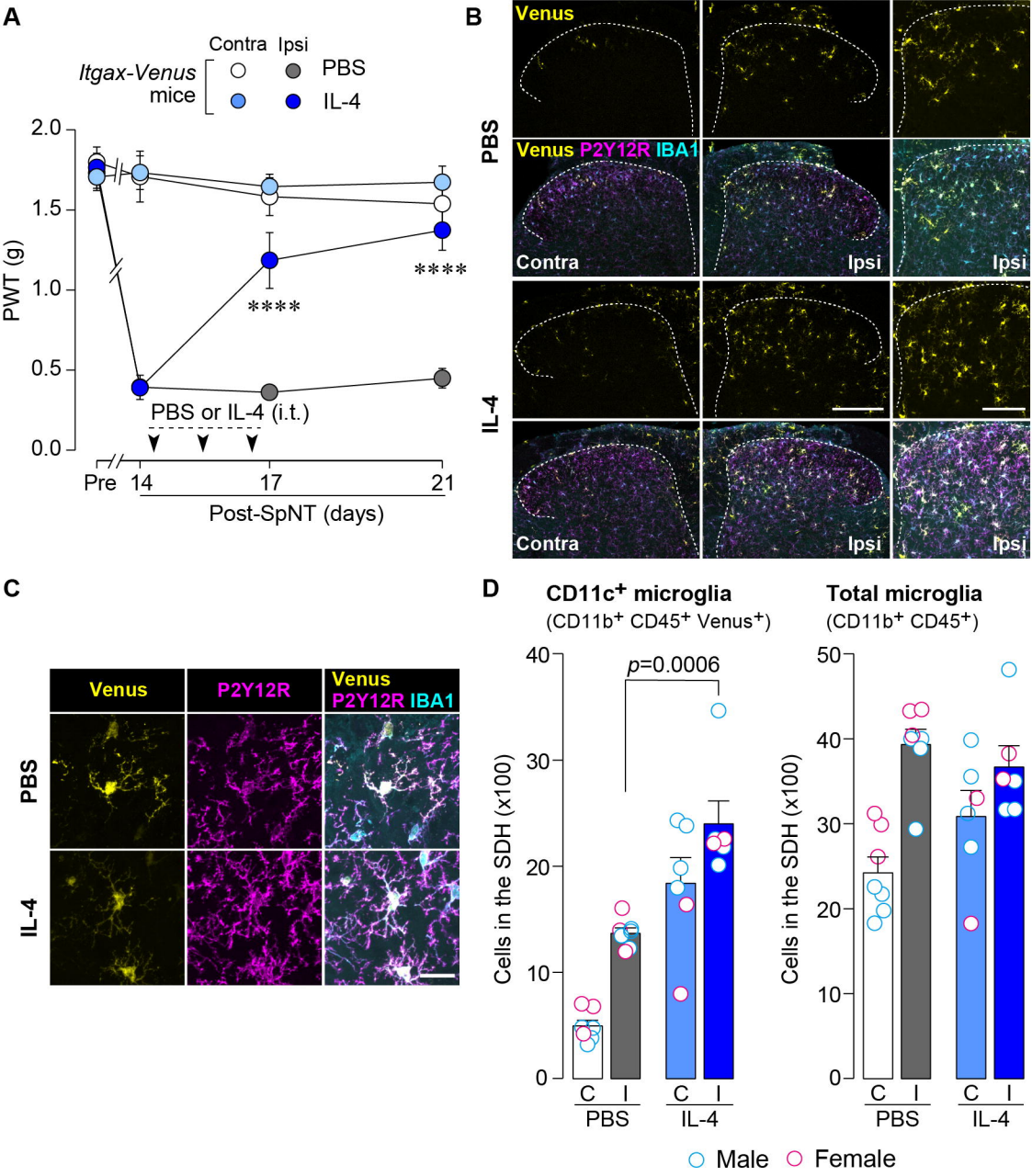
A
Contra Ipsi
Itgax-Venus mice
PBS
IL-4
PWT (g)
2.0
1.5
1.0
0.5
0.0
****
****
PBS or IL-4 (i.t.)
Pre 14 17 21
Post-SpNT (days)
B
Venus
Venus P2Y12R IBA1
PBS
IL-4
Contra
Ipsi
C
Venus
P2Y12R
Venus P2Y12R IBA1
PBS
IL-4
D
CD11c+ microglia
(CD11b+ CD45+ Venus+)
Total microglia
(CD11b+ CD45+)
p=0.0006
Cells in the SDH (x100)
C I C I
PBS IL-4
Male Female

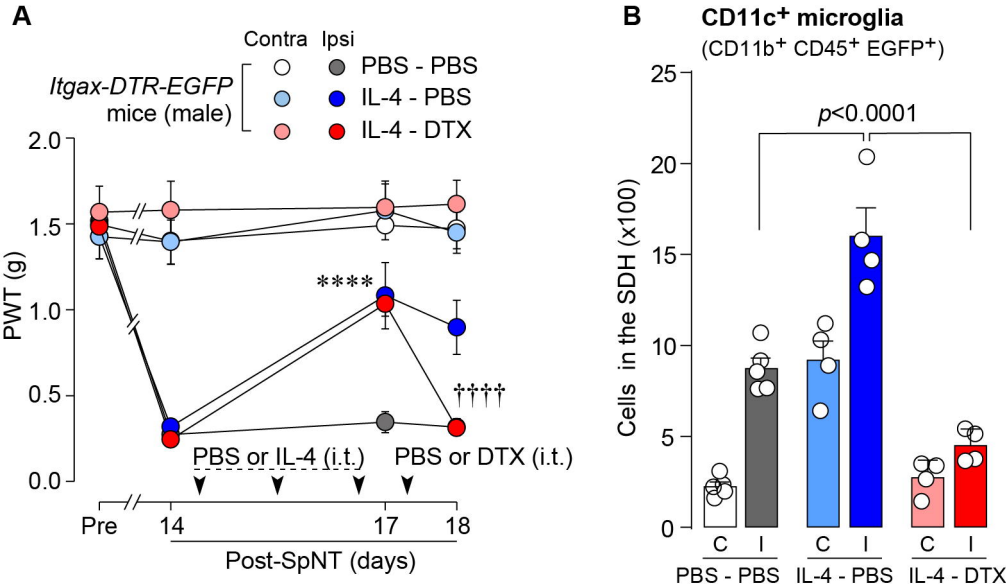
A
Contra Ipsi
Itgax-DTR-EGFP mice (male)
PBS - PBS
IL-4 - PBS
IL-4 - DTX
PWT (g)
2.0
1.5
1.0
0.5
0.0
****
††††
PBS or IL-4 (i.t.)
PBS or DTX (i.t.)
Pre
14
17
18
Post-SpNT (days)
B
CD11c+ microglia
(CD11b+ CD45+ EGFP+)
p<0.0001
Cells in the SDH (x100)
25
20
15
10
5
0
C
I
PBS - PBS
IL-4 - PBS
IL-4 - DTX

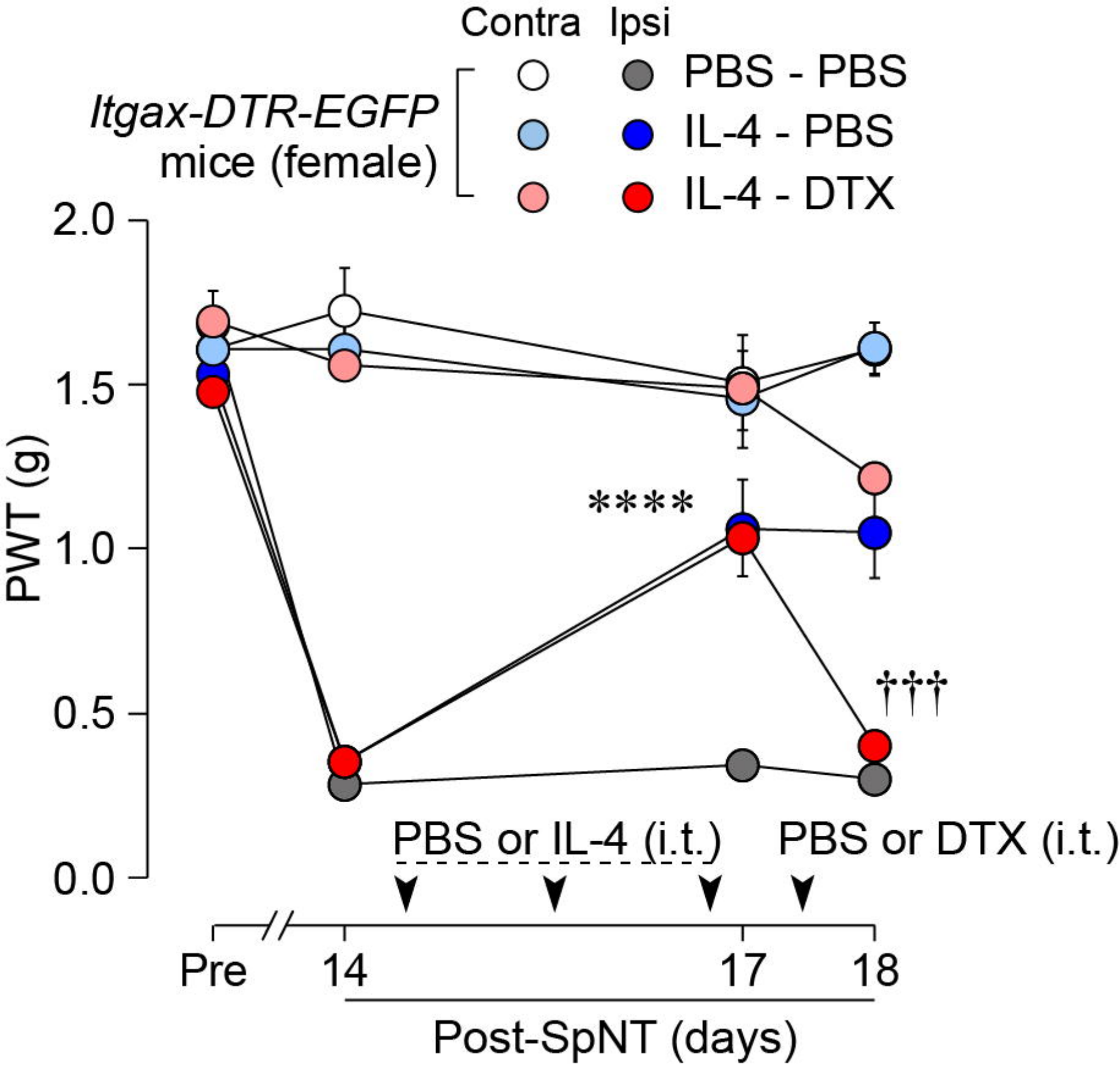
Contra
Ipsi
PBS - PBS
IL-4 - PBS
IL-4 - DTX
Itgax-DTR-EGFP
mice (female)
2.0
1.5
1.0
0.5
0.0
PWT (g)
****
†††
PBS or IL-4 (i.t.)
PBS or DTX (i.t.)
Pre
14
17
18
Post-SpNT (days)

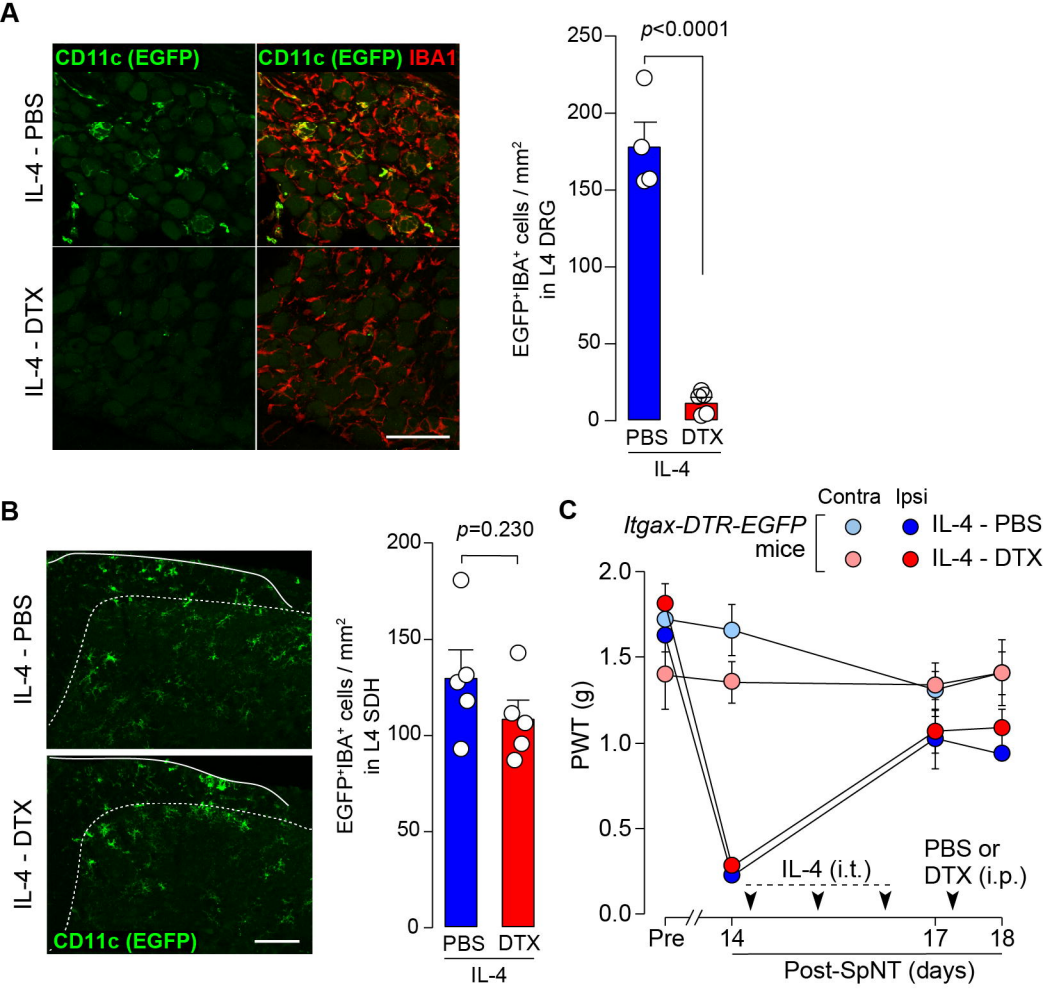
A
CD11c (EGFP)
CD11c (EGFP) IBA1
IL-4 - PBS
IL-4 - DTX
p<0.0001
EGFP+IBA+ cells / mm2 in L4 DRG
250
200
150
100
50
0
PBS
DTX
IL-4
B
IL-4 - PBS
IL-4 - DTX
CD11c (EGFP)
p=0.230
EGFP+IBA+ cells / mm2 in L4 SDH
200
150
100
50
0
PBS
DTX
IL-4
C
Contra
Ipsi
Itgax-DTR-EGFP mice
IL-4 - PBS
IL-4 - DTX
PWT (g)
2.0
1.5
1.0
0.5
0.0
IL-4 (i.t.)
PBS or DTX (i.p.)
Pre
14
17
18
Post-SpNT (days)

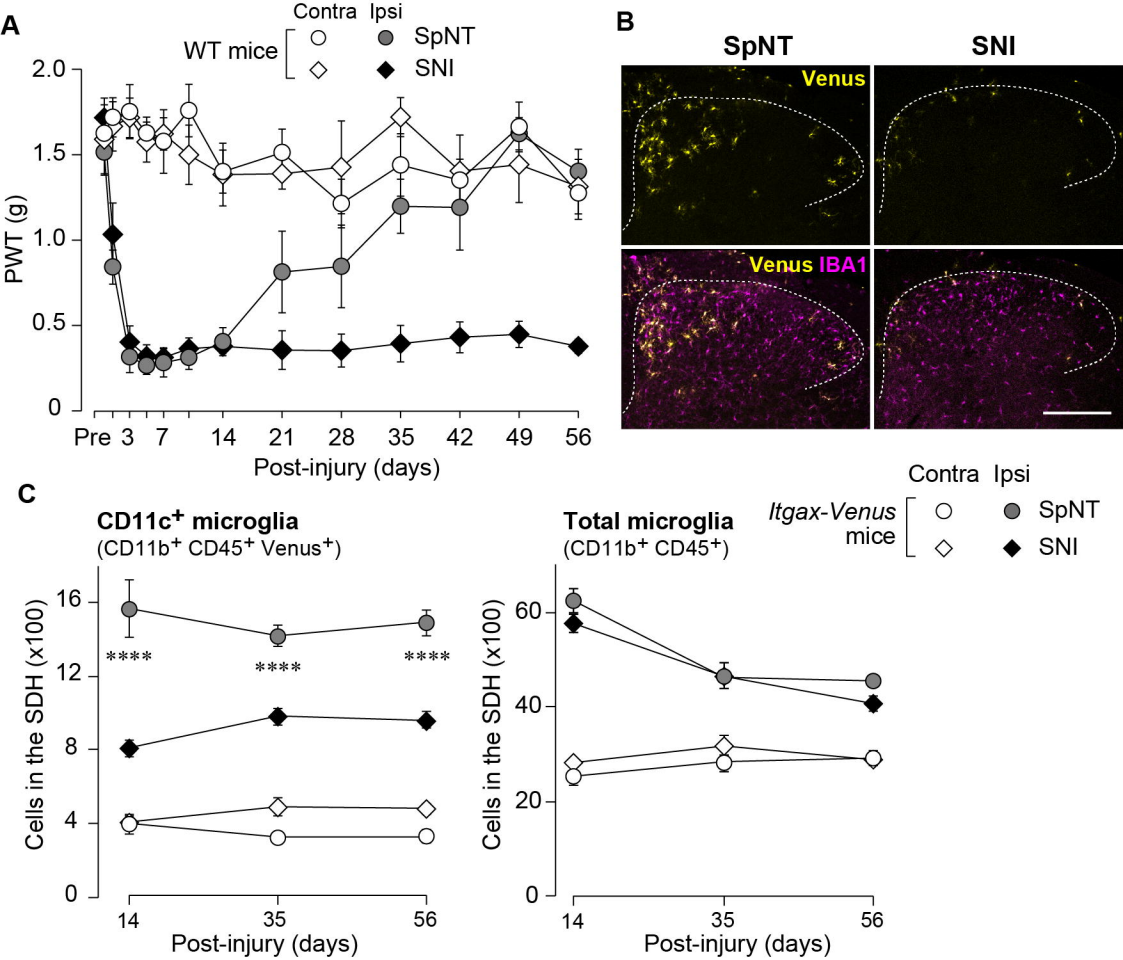
A
Contra Ipsi
WT mice
SpNT
SNI
PWT (g)
2.0
1.5
1.0
0.5
0
Pre 3 7 14 21 28 35 42 49 56
Post-injury (days)
B
SpNT
SNI
Venus
Venus IBA1
C
CD11c+ microglia
(CD11b+ CD45+ Venus+)
Total microglia
(CD11b+ CD45+)
Itgax-Venus mice
Contra Ipsi
SpNT
SNI
Cells in the SDH (x100)
16
12
8
4
0
****
****
****
14 35 56
Post-injury (days)
60
40
20
0
14 35 56
Post-injury (days)

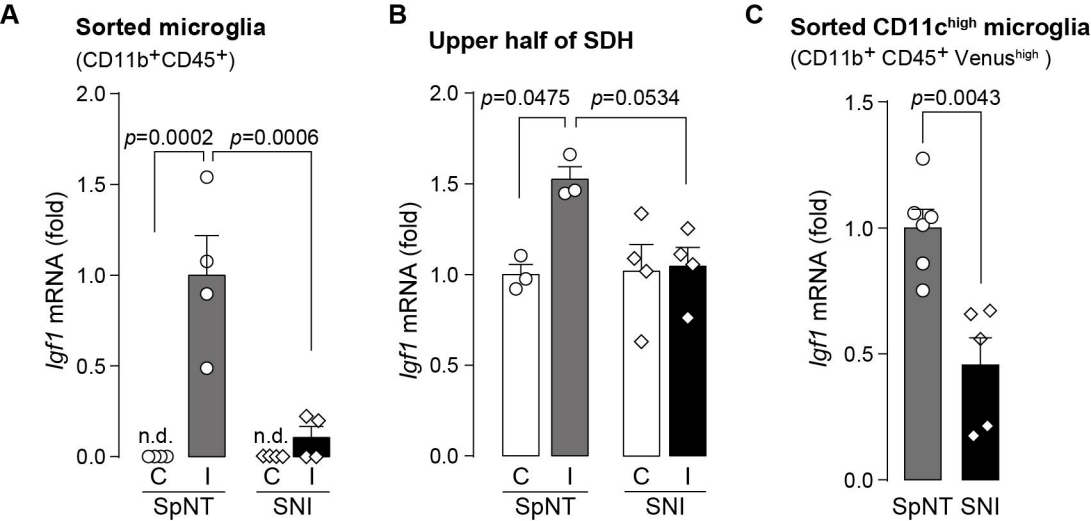
A
Sorted microglia
(CD11b+CD45+)
p=0.0002
p=0.0006
Igf1 mRNA (fold)
2.0
1.5
1.0
0.5
0.0
n.d.
n.d.
C
I
C
I
SpNT
SNI
B
Upper half of SDH
p=0.0475
p=0.0534
Igf1 mRNA (fold)
2.0
1.5
1.0
0.5
0.0
C
I
C
I
SpNT
SNI
C
Sorted CD11chigh microglia
(CD11b+ CD45+ Venushigh)
p=0.0043
Igf1 mRNA (fold)
1.5
1.0
0.5
0.0
SpNT
SNI

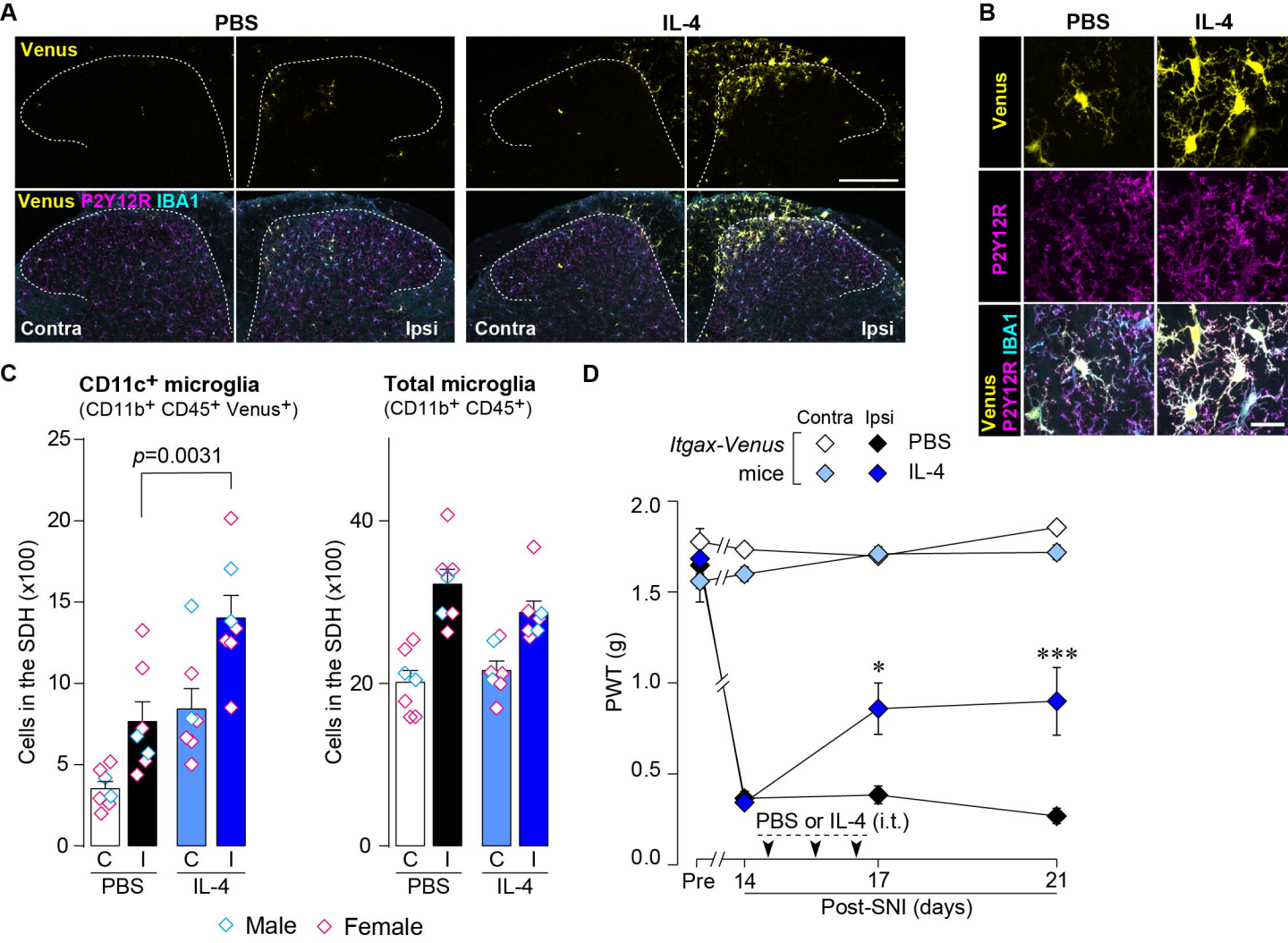
A
PBS
IL-4
Venus
Venus P2Y12R IBA1
Contra
Ipsi
B
PBS
IL-4
Venus
P2Y12R
Venus P2Y12R IBA1
C
CD11c+ microglia
(CD11b+ CD45+ Venus+)
Total microglia
(CD11b+ CD45+)
p=0.0031
Cells in the SDH (x100)
C I C I
PBS IL-4
Male
Female
D
Contra Ipsi
Itgax-Venus mice
PBS
IL-4
PWT (g)
*
***
PBS or IL-4 (i.t.)
Pre 14 17 21
Post-SNI (days)

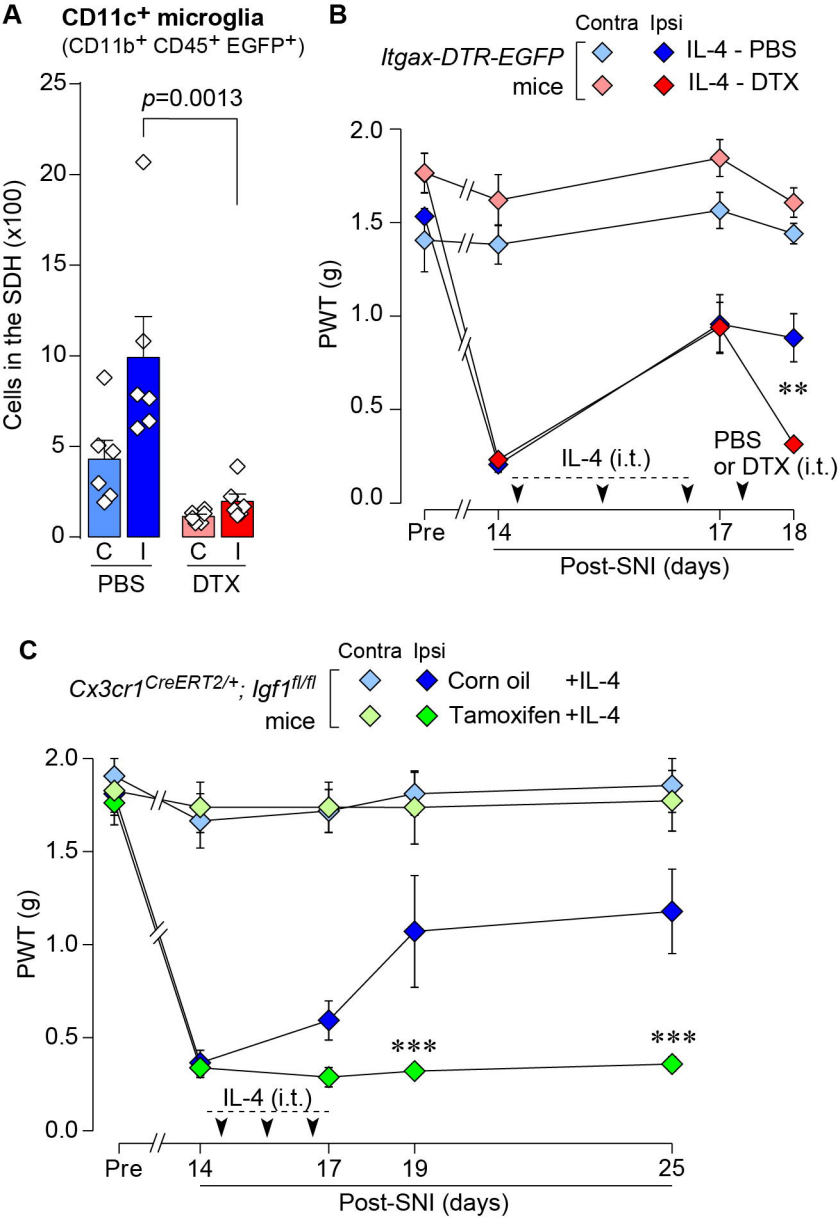
A
CD11c+ microglia
(CD11b+ CD45+ EGFP+)
p=0.0013
Cells in the SDH (x100)
25
20
15
10
5
0
C
I
C
I
PBS
DTX
B
Contra Ipsi
Itgax-DTR-EGFP mice
IL-4 - PBS
IL-4 - DTX
PWT (g)
2.0
1.5
1.0
0.5
0.0
**
IL-4 (i.t.)
PBS or DTX (i.t.)
Pre
14
17
18
Post-SNI (days)
C
Contra Ipsi
Cx3cr1CreERT2/+; Igf1fl/fl mice
Corn oil +IL-4
Tamoxifen +IL-4
PWT (g)
2.0
1.5
1.0
0.5
0.0
***
***
IL-4 (i.t.)
Pre
14
17
19
25
Post-SNI (days)